IEEE Photonics Journal
An IEEE Photonics Society Publication

Open Access

Polarization Multiplexing Silicon-Photonic Optical Phased Array for 2D Wide-Angle Optical Beam Steering

Volume 13, Number 2, April 2021

Xibo Yan
Jingye Chen
Daoxin Dai
Yaocheng Shi

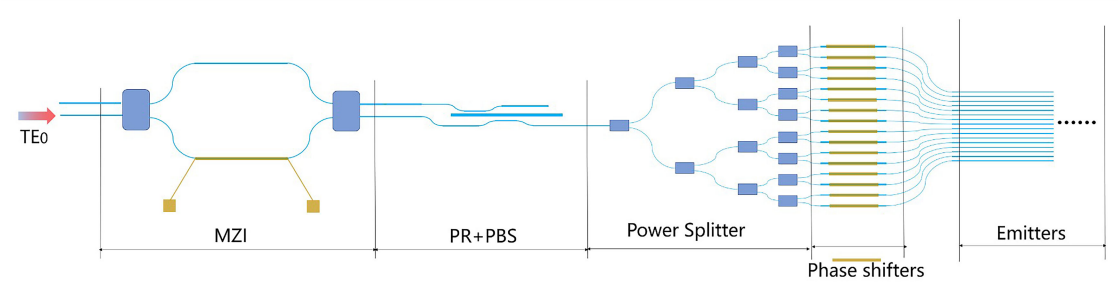

DOI: 10.1109/JPHOT.2021.3058667

IEEE photonics SOCIETY
IEEE

Polarization Multiplexing Silicon-Photonic Optical Phased Array for 2D Wide-Angle Optical Beam Steering

Xibo Yan,[1,2] **Jingye Chen**[1,2] **Daoxin Dai**[1,2] **and Yaocheng Shi**[1,2]

[1]Center for Optical and Electromagnetic Research, State Key Laboratory for Modern Optical Instrumentation, College of Optical Science and Engineering, Zhejiang University, Hangzhou 310058, China
[2]Ningbo Research Institute, Zhejiang University, Ningbo 315100, China

DOI:10.1109/JPHOT.2021.3058667

Manuscript received January 4, 2021; revised February 5, 2021; accepted February 8, 2021. Date of publication February 11, 2021; date of current version March 3, 2021. This work was supported in part by the National Natural Science Foundation of China (61922070), and in part the Fundamental Research Funds for the Central Universities. Corresponding author: Jingye Chen (e-mail: jingyechen@zju.edu.cn).

Abstract: We propose the silicon photonic optical phased array (OPA) with large scanning angle by using polarization multiplexing. A Mach-Zehnder interferometer (MZI) switch together with a polarization splitter/rotator is utilized to select the polarization mode input to the OPA. By optimizing the OPA grating emitter, the steering angle can be doubled with the input of the TE/TM polarization modes. An 1×16 silicon-based optical phased array with polarization multiplexing is designed as an example. The simulation results show that 77.4° lateral beam steering with no sidelobes via phase tuning and 28.2° longitudinal beam steering via wavelength tuning can be realized.

Index Terms: Optical phased array, polarization multiplexing, photonic integrated circuits.

1. Introduction

The integrated optical phased array (OPA) has been extensively studied due to its solid-state beam steering capability, which is a good prospect in the fields of light detection and ranging (LiDAR), free space optical communications, and also laser display [1]–[3]. The OPA based LiDAR has the advantages of low cost, high stability, and easy for monolithic optoelectronic integration [1]. In current integrated OPA, although the size of the array and the number of elements continue to increase [4]–[5], the beam quality and the steering angles are still limited [6]. In order to realize the angular steering of the OPA in two-dimensional (2D) space, currently there are two main methods: one is to directly realize the OPA emitter arranged in a 2D array [7]; the other is to tune the scanning wavelength with the one-dimensional (1D) grating array to achieve the 2D steering. For the OPA with 2D emitter array, it will be difficult to achieve a large beam steering angle since the pitch of the emitter array cannot be too small due to the crosstalk [8]. Thus, 1D grating array together with wavelength tuning is mostly adopted to realize the 2D beam steering. Regarding the beam steering in the longitudinal dimension, the steering range will be limited by the wavelength tuning range of the tunable laser source. A tunable laser with the 100nm tuning range can generally achieve a

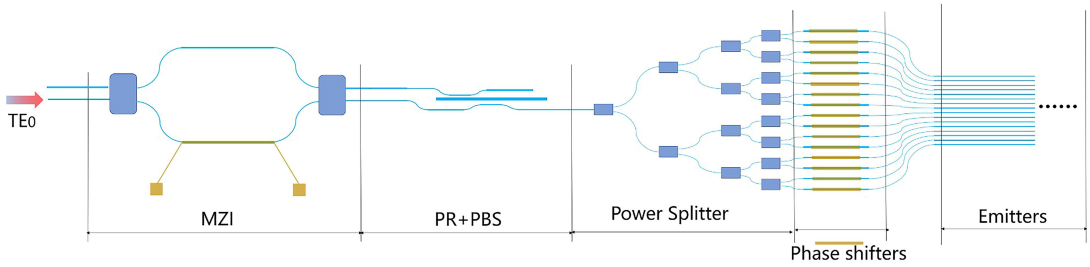

Fig. 1. The schematic of the proposed polarization multiplexed OPA.

beam steering angle of ∼14° [9]–[12]. There is also longitudinal beam steering by thermo-optical tuning of the grating emitter area, but the steering angle can only reach 10° [13].

In this paper, we propose a 2D OPA with large steering angles by utilizing polarization multiplexing [12]. The polarization mode selection is realized by using a Mach-Zehnder interferometer (MZI) based switch combined with a polarization splitter/rotator [14]. Thus, the scanning angle of the OPA emitter can be expanded by switching between the two polarizations as the input of the OPA. The 2D OPA with 16 silicon waveguide arrays is designed as an example. The simulation results show that the longitudinal steering angle can reach 28.2° through the polarization multiplexing. While the lateral steering angle can maintain as large as 77.4° by using the phase tuning with a waveguide pitch down to 1.2 μm.

2. Design and Analysis

The schematic of the proposed polarization multiplexed OPA is shown in Fig. 1. The designed OPA can be divided into two parts: the polarization selection section and the OPA section. The polarization selection section composes of a switch based on MZI and a polarization splitter/rotator (PSR), which is used to switch between the two polarizations. For the OPA section, it consists of 1 $\times$ N power splitters, N phase shifters and the grating emitters.

The 2D beam steering is realized by combining the phase tuning and the wavelength tuning. We expect to use the polarization multiplexing to expand the longitudinal steering beam angle. When the wavelength of the input light is tuned, the output angle for the grating emitter will be changed accordingly. Thus, the longitudinal beam steering properties are mostly determined by the structure of the grating emitters. The grating emitters based on silicon-on-insulator (SOI) waveguides are usually polarization sensitive. Thus, the longitudinal beam steering range of the OPA is aimed to be doubled if the steering angles for the two polarizations can be fully utilized. To ensure the working wavelength around 1550nm and also the fabrication feasibility, the parameters for the grating emitters are chosen as follows: grating period of 800 nm, etching depth of 70 nm, and duty cycle of 0.5. The scanning angle for the grating emitter is determined by the following equation:

$$\sin\theta = \frac{\Lambda n_{\text{eff}} - \lambda_0}{n_{\text{ct}}\Lambda}. \tag{1}$$

where Λ is the period of the grating, λ is the freespace wavelength, n_{eff} the effective index of the guided mode, and n_{ct} the refractive index of the background, which is the air in this case. The beam scanning ranges of the fundamental TE mode and TM mode are calculated for the grating emitters with waveguide width $w = 400$ nm and different silicon thickness h (most often used ones: 220 nm, 250 nm, 300 nm, 340 nm) and the obtained results are shown in Fig. 2. With the increase of the silicon thickness, the beam steering ranges of the two polarization modes gradually approach each other. The reason for this is the refractive index difference of the two polarizations will reduce with the increase of the silicon thickness. From Fig. 2(d), one may find that the steering angle for the TE fundamental mode is adjacent to that of the TM fundamental mode for the grating emitter with

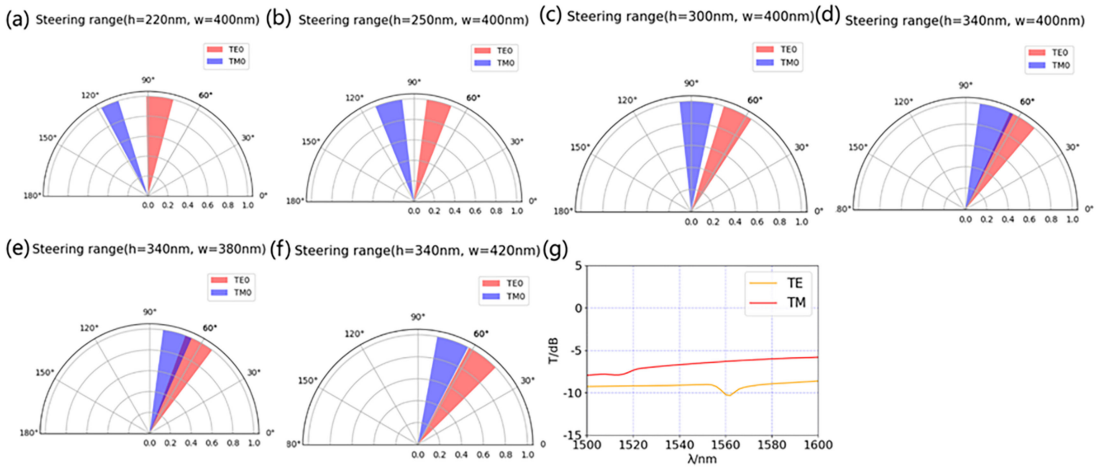

Fig. 2. Scanning range of gratings of different heights in two polarization modes. (a) 220 nm, w = 400 nm. (b) 250 nm, w = 400 nm. (c) 300 nm, w = 400 nm. (d) 340 nm, w = 400 nm. (e) 340 nm, w = 380 nm. (f) 340 nm, w = 420 nm. (g) The emission efficiency of the grating.

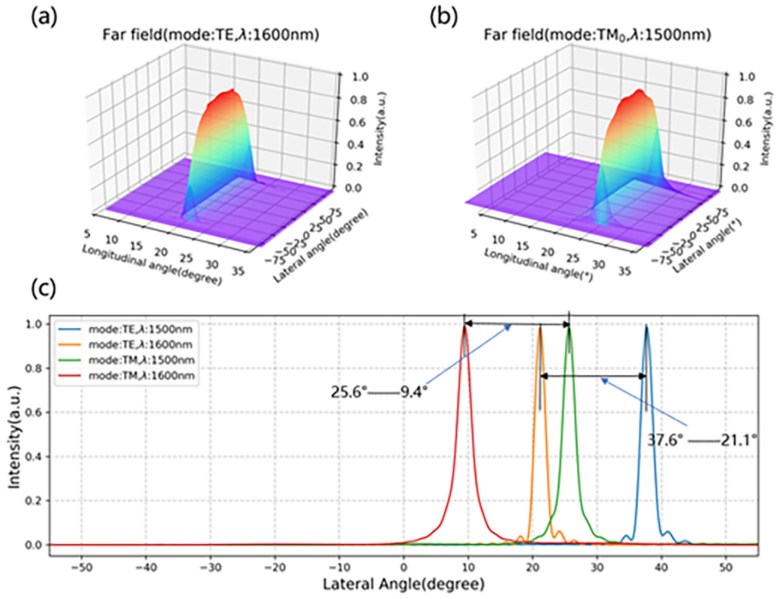

Fig 3. (a) Far field of 1600 nm TE fundamental mode. (b) Far field of 1500 nm TM fundamental mode. (c) Beam steering range of 340 nm SOI grating emitter in two polarization modes.

a silicon thickness of 340 nm. Within 20 nm variation of the waveguide width, the grating emitter can achieve continuous field of view with TE_0 and TM_0 in the range of 1500 nm to 1600 nm. The steering angle for TE mode is from 37.6° to 21.1°, while the steering angle for TM mode is from 25.6° to 9.4° with a scanning wavelength range from 1500–1600nm. It is clearly showing that the scanning range can be almost doubled compared to the OPA working at a single polarization. The Fig. 2(g) show the emission efficiency of the grating, which is about 12.6%.The calculated far field distribution and the steering angle are shown in Fig. 3.

To ensure an efficient on-chip polarization switching, a polarization selection section is designed to switch between the two polarization modes. The polarization selection section consists of a MZI switch [14], [15], a polarization rotator (PR) and a polarization splitter (PBS). Fig. 4 shows the detailed structure of the polarization selection. The MZI switch is utilized to select the output from

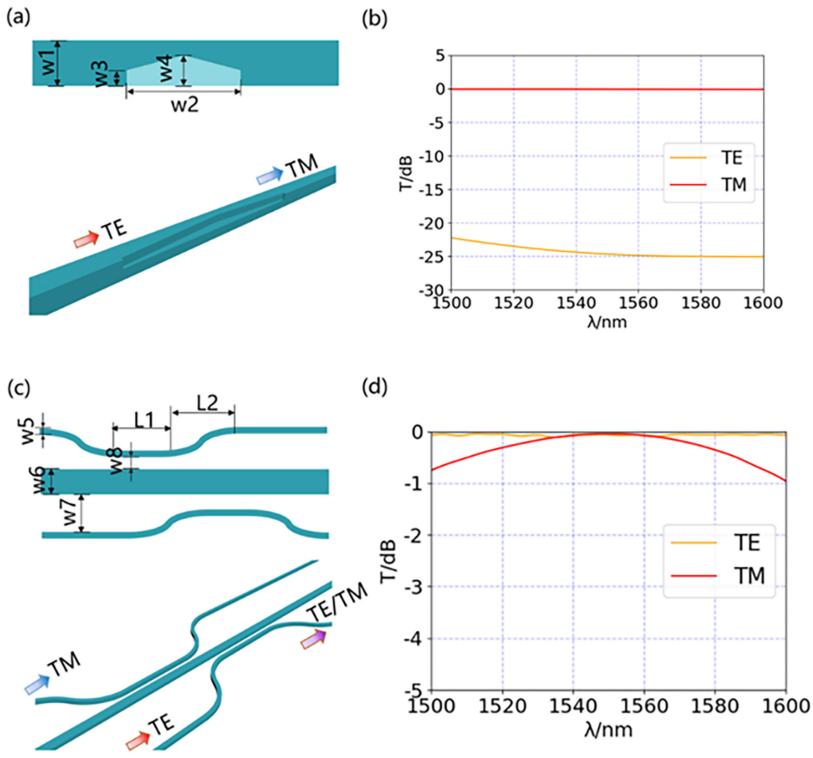

Fig 4. (a) 2D top view and 3D diagram of the polarization rotator. (b) Calculated transmittance spectra of PR for TE to TM over 1500–1600 nm wavelength range. (c) 2D top view and 3D diagram of the polarization beam splitter. (d) Calculated transmittance spectra of PBS for TM /TE over 1500–1600 nm wavelength range.

the two ports, and it has an extinction ratio of $>$20 dB within 1500-1600 nm. A pentagonal groove structure is utilized to realize the polarization rotation with a large enough working bandwidth [16]. The designed parameters are as follows: $w_1 = 350$ nm, $w_2 = 4.7$ μm, $w_3 = 50$ nm, $w_4 = 150$ nm. The etching depth of the groove is 150 nm. A three-waveguide asymmetric coupler [18] is used to realize the polarization beam splitting. When the TE_0 input mode is launched and output from the upper port of the MZI switch, it will output from the PSR as the TE_0 mode. While if a π phase shift is applied to the MZI switch, the TE_0 input mode will output from the lower port of the MZI switch and then converted to be TM_0 mode by the PR. With such a configuration, the two polarizations can be then selected as the input for the cascaded OPA. Fig. 4(a) and (c) shows the diagram of the polarization rotator and the polarization beam splitter. The detailed parameters are as follows: $w_5 = 340$ nm, $w_6 = 830$ nm, $w_7 = 2.2$ μm, $w_8 = 200$ nm, $L_1 = 8.2$ μm, $L_2 = 10$ μm. Fig. 4(b) and (d) show the calculated transmission transmittance spectra for the PR and PBS, respectively. The PR has an extinction ratio of $>$22 dB in 100 nm wavelength band. Low loss can be achieved over a large 1 dB bandwidth over 100 nm.

The phase tuning is applied to achieve the beam steering in the lateral direction. The intervals between the emitter waveguide arrays are important for the steering properties. When the interval is larger than $\lambda/2$, typical unwanted side lobes will be generated [17]. However, smaller interval may introduce crosstalk. For one-dimensional steering waveguide arrays, waveguides of different widths can be alternately arranged to reduce the crosstalk, thereby reducing the interval and enabling a wide range of lateral steering angles [18].The OPA formed by using a grating emitter array can also expand its lateral scanning range in the same way, but grating emitters of different widths need to be designed with different parameters to maintain the same emitting angle [19]. For different wavelength, the emitting angle of different gratings will be different which will limit its angular range

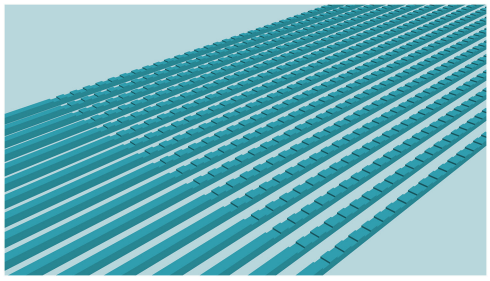

Fig. 5. The schematic of the grating emitter.

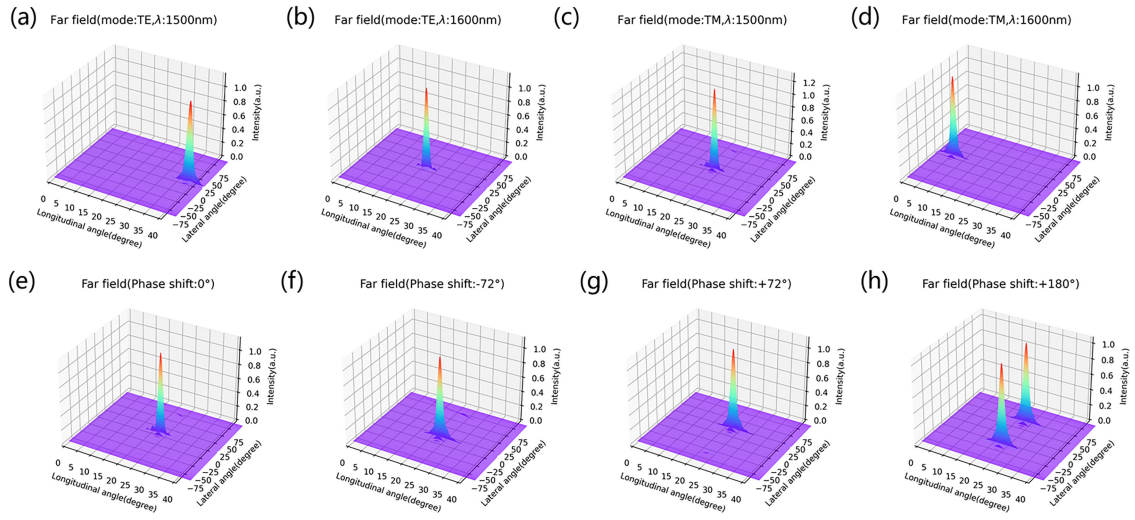

Fig. 6. (a–d) The far field distribution for the OPA at different working wavelength (longitudinal steering, the phase shift remains at 0°). (e–h) The far field distribution for the OPA at different phase shift (lateral steering, the working wavelength remains at 1550 nm).

in the longitudinal steering dimension. In order to achieve a larger lateral steering angle for OPA, the interval between the waveguides should be as small as possible. Thus, a uniform waveguide array with an interval of 1.2 μm is utilized in our design. With such design, a relatively large steering angle without sidelobes can be achieved and the crosstalk of the grating array is less than 30 dB. Fig. 5 shows the schematic of the grating emitter array. 3D FDTD is performed to calculate the beam steering property of the whole OPA. The calculated results show that the maximum steering range in the lateral direction is $-38.7°$ to $38.7°$. The calculated far field distribution is shown in the Fig. 6, with the smallest lateral beam width of $\sim 4°$ and an average longitudinal beam width of $\sim 2°$. The emission efficiency of the grating coupler can be improved by adding a metal reflector or distributed Bragg reflector (DBR) underneath the grating emitter [20], [21]. The calculated loss of the entire OPA system is about 11.3 dB (0.5 dB from the MZI switch, 0.6 dB from PR, 0.6 dB from PBS, 1.2 dB from MMI couplers and 9 dB from the grating emitter), which can be optimized further.

3. Conclusion

In conclusion, we proposed a design of a polarization multiplexed silicon-based 2D optical phased array. A polarization selection section consists of a MZI, a PR, and a PBS is utilized to achieve efficient switching of the output polarization mode. In application, the OPA firstly has a polarization selection with the MZI switch, then the phase of thermo-optical phase shifters will be controlled for lateral beam steering and the wavelength will be controlled with a tunable laser for longitudinal

beam steering. With such a design, the scanning angle in the longitudinal direction extends by nearly twice to the one working at one polarization state. A 2D OPA with 16 waveguide arrays is designed as an example. The calculation results show that a steering angle of $77.4^\circ \times 28.2^\circ$ can be achieved and can be extended by larger range of wavelength tuning. We believe that it has the potential application in the on-chip OPA.

References

[1] M. Heck, "Highly integrated optical phased arrays: Photonic integrated circuits for optical beam shaping and beam steering," *Nanophotonics*, vol. 6, no. 1, pp. 93–107, 2017.

[2] C. Poulton *et al.*, "Coherent solid-state LIDAR with silicon photonic optical phased arrays," *Opt. Lett.*, vol. 42, pp. 4091–4094, 2017.

[3] Y. Kohno, K. Komatsu, R. Tang, Y. Ozeki, Y. Nakano, and T. Tanemura, "Ghost imaging using a large-scale silicon photonic phased array chip," *Opt. Exp.*, vol. 27, pp. 3817–3823, 2019.

[4] S. Miller *et al.*, "512-element actively steered silicon phased array for low-power LIDAR," in *Proc. Conf. Lasers Electro-Opt., OSA Tech. Dig.*, 2018, Paper JTh5C.2.

[5] S. Miller *et al.*, "Large-scale optical phased array using a low-power multi-pass silicon photonic platform," *Optica*, vol. 7, pp. 3–6, 2020.

[6] D. Hutchison *et al.*, "High-resolution aliasing-free optical beam steering," *Optica*, vol. 3, pp. 887–890, 2016.

[7] J. Sun, E. Timurdogan, and A. Yaacobi, "Large-scale nanophotonic phased array," *Nature*, vol. 493, pp. 195–199, 2013.

[8] H. Abediasl and H. Hashemi, "Monolithic optical phased-array transceiver in a standard SOI CMOS process," *Opt. Exp.*, vol. 23, pp. 6509–6519, 2015.

[9] K. Van Acoleyen, W. Bogaerts, J. Jágerská, N. L. Thomas, R. Houdré, and R. Baets, "Off-chip beam steering with a one-dimensional optical phased array on silicon-on-insulator," *Opt. Lett.*, vol. 34, pp. 1477–1479, 2009.

[10] J. Doylend, M. Heck, J. Bovington, J. Peters, L. Coldren, and J. Bowers, "Two-dimensional free-space beam steering with an optical phased array on silicon-on-insulator," *Opt. Exp.*, vol. 19, pp. 21595–21604, 2011.

[11] D. Kwong *et al.*, "On-chip silicon optical phased array for two-dimensional beam steering," *Opt. Lett.*, vol. 39, pp. 941–944, 2014.

[12] Y. Zeng, S. Qu, and J. Wu, "Polarization-division and spatial-division shared-aperture nanopatch antenna arrays for wide-angle optical beam scanning," *Opt. Exp.*, vol. 28, pp. 12805–12826, 2020.

[13] S. Kim *et al.*, "Thermo-optic control of the longitudinal radiation angle in a silicon-based optical phased array," *Opt. Lett.*, vol. 44, pp. 411–414, 2019.

[14] Y. Zhang, Y. He, Q. Zhu, C. Qiu, and Y. Su, "On-chip silicon photonic 2×2 mode- and polarization-selective switch with low inter-modal crosstalk," *Photon. Res.*, vol. 5, pp. 521–526, 2017.

[15] S. Wang and D. Dai, "Polarization-insensitive 2×2 thermo-optic Mach–Zehnder switch on silicon," *Opt. Lett.*, vol. 43, pp. 2531–2534, 2018.

[16] D.D. Z. Wang, "Ultrasmall Si-nanowire-based polarization rotator," *J. Opt. Soc. Amer. B*, vol. 25, no. 5, pp. 747–753, 2008.

[17] G. Zhou, S. Qu, and J. Wu, "Grating lobe suppression in optical phased arrays by loading near-wavelength grating," *Opt. Lett.*, vol. 45, pp. 5664–5667, 2020.

[18] C. Li and D. Dai, "Compact polarization beam splitter based on a three-waveguide asymmetric coupler with a 340-nm-Thick silicon core layer," *J. Lightw. Technol.*, vol. 36, pp. 2129–2134, 2018.

[19] C. Phare, M. Shin, J. Sharma, S. Ahasan, H. Krishnaswamy, and M. Lipson, "Silicon optical phased array with grating lobe-free beam formation over 180 degree field of view," in *Proc. Conf. Lasers Electro-Opt., OSA Tech. Dig.*, 2018, Paper SM3I.2.

[20] S. Romero-García, F. Merget, F. Zhong, H. Finkelstein, and J. Witzens, "Visible wavelength silicon nitride focusing grating coupler with AlCu/TiN reflector," *Opt. Lett.*, vol. 38, pp. 2521–2523, 2013.

[21] Y. Zhang *et al.*, "Sub-wavelength-pitch silicon-photonic optical phased array for large field-of-regard coherent optical beam steering," *Opt. Exp.*, vol. 27, pp. 1929–1940, 2019.